ELSEVIER

Ceramics International 27 (2001) 859–863

CERAMICS INTERNATIONAL

www.elsevier.com/locate/ceramint

Electrical conductivity of sol–gel derived yttria-stabilized zirconia

Vladimir V. Srdić*, Radovan P. Omorjan

Faculty of Technology, University of Novi Sad, Novi Sad, Yugoslavia

Received 18 December 2000; received in revised form 20 March 2001; accepted 25 March 2001

Abstract

A 3 mol% Y_2O_3 zirconia stabilized powder has been synthesized by destabilization of an aqueous zirconia sol prepared by the alkoxide hydrolysis method. The powder calcined at 500°C is ultrafine with tetragonal crystallites of about 8 nm, slightly agglomerated and with a narrow pore size distribution having an average pore size of 5.2 nm. Zirconia ceramics with density higher than 92%TD and grain size on the order of 100 nm have been obtained by uniaxial pressing at 500 MPa and vacuum sintering at 1000°C. Electrical conductivity of sintered samples, evaluated by complex impedance spectroscopy measurements, indicated that the zirconia stabilized with 3 mol% Y_2O_3 can potentially be used as an oxygen semipermeable dense membrane, but only at a relatively high temperature.

Keywords: A. Sol–gel processes; B. Electrical conductivity; Yttria-stabilized zirconia

1. Introduction

Oxide materials with significant oxygen ionic conductivity have a wide application in high-temperature electrochemical devices such as solid oxide fuel cells (SOFCs), oxygen pumps, oxygen sensors, oxygen separation membranes and membrane reactors for hydrocarbon partial oxidation. These solid electrolyte materials should have a high ionic conductivity at the operating temperature, desirable stability in both oxidizing and reducing atmospheres and absence of the transport property degradation with time.

Yttrium-stabilized zirconia is one of the most used solid electrolyte in oxygen-ion conducting devices [1,2]. Stabilization of the tetragonal or cubic zirconia in this system is obtained by substitution of Zr^{4+} with Y^{3+} ions, maintaining local charge balance with the creation of one oxygen vacancy for every two Y^{3+} ions introduced. Formation of a large concentration of oxygen vacancies is very important as oxygen-ion conduction takes place by movement of oxygen ions via these vacancies. The bulk component of the total conductivity depends mainly on the yttrium amount and is maximal when the Y_2O_3 concentration is close to 9.5 mol% [2]. The grain-boundary component of the total conductivity depends also on the Y_2O_3 content, but it is more strongly related to the microstructure (grain size and density) [3–5] and grain-boundary structure determined by the type and amount of impurities [6]. Different processing techniques (including powder synthesis, compaction and pellet sintering) have been used to modify the microstructure of Y–TZP and grain-boundaries in order to increase oxygen-ion transport. In this paper zirconia doped with 3 mol% Y_2O_3 (3Y–TZP) nanopowder was synthesized by destabilization of an aqueous zirconia sol prepared by hydrolysis of zirconium-alkoxide (and yttrium-chloride). Air and vacuum sintering were performed to produce a dense, gas-tight zirconia ceramic. Conductivity of sintered samples was evaluated by complex impedance spectroscopy measurements.

2. Experimental

2.1. Sample preparation

Zirconia doped with 3 mol% Y_2O_3 nanopowder was synthesized by hydrolysis of $Zr(OC_3H_7)_4$ (Fluka, Switzerland) dissolved in anhydrous ethanol with distilled water (from highly diluted ethanol solution of YCl_3 (Merck, Germany) and H_2O), under acidic condition (pH ~ 1) and at room temperature (alkoxide, water and

* Corresponding author. Tel.: +381-21-450-288; fax: +381-21-450-413.

E-mail address: srdicvv@uns.ns.ac.yu (V.V. Srdić).

0272-8842/01/$20.00
PII: S0272-8842(01)00041-4

hydrochloric acid molar ratio was 1:2:0.5). An aqueous sol was obtained by continuous evaporation and replacing the ethanol with distilled water without changing the concentration and pH. The hydroxides were precipitated by slowly adding this aqueous sol to a well-stirred ammonium hydroxide solution (pH > 11). The precipitated powder was washed with distilled water until there was no indication of residual Cl^- (qualitatively determined by adding a few drops of the wash effluent to a $AgNO_3$ solution), and then three times with absolute ethanol to remove free water and replace the particle surface hydroxyl with ethoxy groups [7]. After washing, the gel nanopowder was filtered, dried at 120°C for 1 day and calcined at 500°C for 1 h.

The calcined powder was dry milled with yttrium-stabilized zirconia balls (TOSOH), uniaxially pressed at 500 MPa in a hard metal die with a diameter of 8 mm, at room temperature. The pressed pellets were heated with a heating rate of 5°C/min, held at 500°C for 1 h and than pressureless sintered in air or in vacuum (0.5 Pa) at different temperatures up to 1070°C.

2.2. Characterization

The specific surface area of the as-synthesized and calcined 3Y–TZP powders was measured by nitrogen adsorption according to the BET method using a Micromeritics ASAP 2400 instrument. The particle size was calculated assuming spherically shaped particles by $d_{BET} = 6/(\rho S_v)$, where ρ is the density and S_v the specific surface area of the sample. The X-ray diffraction measurements were performed using a Philips PW 1050 instrument with CuK_α radiation. Zirconia phases were identified by comparison of the X-ray diffractograms with the JCPDS database. The crystallite size was estimated from the (111) reflection of the tetragonal phase using the Scherrer equation ($d = 0.9\lambda/\beta\cos\theta$, where λ is the wavelength of the radiation, β full width at half maximum and θ the scattering angle) after subtracting the instrumental broadening [8]. The density of the pressed and sintered pellets was measured from the geometry and the mass of the sample. The pore size distribution of the 3Y–TZP samples was measured by the nitrogen adsorption and determined according to the BJH theory from the adsorption isotherm [9]. The average grain size was estimated from SEM micrographs recorded with a high resolution scanning electron microscope (HRSEM Philips XS 30) operating at 20 kV.

2.3. Conductivity measurement

The a.c. conductivity (as a function of temperature) of the sintered 3Y–TZP pellets was measured in air by the pseudo four-probe impedance spectroscopy [10]. Measurements were made with a Hewlett Packard HP 4284A and HP 4285A impedance analyzers from 20 Hz to 3 MHz in temperature range 75–825°C (total of 25 experimental points). Electrodes were obtained by coating both sides of the 3Y–TZP sample discs with silver paste. Samples were positioned between two silver discs and pressed with a weak mechanical force controlled by a screw/spring system.

3. Results and discussion

3.1. Characterization

Characteristics of the as-synthesized and the calcined ZrO_2–3 mol% Y_2O_3 powder are presented in Table 1. The as-synthesized powder is amorphous, with a high surface area and the average particle size of 3.4 nm, calculated from multipoint BET. The mass loss of 25.1% occurring on heating up to 1000°C is very close to the theoretical value of 22.4%, that corresponds to decomposition of hydroxides to oxides, i.e. $Zr(OH)_4$ to ZrO_2, indicating the character of the as-synthesized powder. During calcination at 500°C for 1 h the as-synthesized powder crystallizes in tetragonal yttria-doped zirconia solid solution and the surface area decreases considerably to 122 m^2/g (Table 1), due to partial sintering, crystallization and particle coarsening. The average crystallite size determined by XRD (7.8 nm) is close to the average particle size of 8.2 nm, calculated from BET, that could be an indication of a relative low degree of agglomeration and/or a significant contribution of strain to the XRD line broadening. The presence of agglomeration is confirmed by the shape of the

Table 1
Powders and green pellet characteristics

	As-synthesized powder	Calcined powder at 500°C	Pellet pressed at 500 MPa
Surface area (m^2/g)	294	122	116
Average particle size (from BET) (nm)	3.4	8.2	–
Phase composition	Amorphous	*t*-ZrO_2	*t*-ZrO_2
Average grain size (from XRD) (nm)	–	7.8	7.5
Mass loss during heating up to 1000°C (%)	25.1	–	–
Green density of pressed pellet (g/cm^3)	–	–	2.41

adsorption/desorption hysteresis loop of the calcined Y–ZrO_2 powder (Fig. 1) and microporosity of the calcined particles (Fig. 2).

The 3Y–TZP pellet uniaxially pressed at 500 MPa has a green density of 39.5%TD (Table 1) and a very fine microstructure with unimodal pore size distribution and the average pore size of 5.2 nm (Fig. 2). The adsorption/desorption hysteresis loop, as an indication of the pore morphology, is predominantly of *type E* [11], indicating tubular capillaries with strongly varying widths, characteristic for a powder compact with a lower agglomeration state [12]. It is interesting to note that the pressed pellet has only a little bit lower specific surface area than the calcined powder (Table 1) and that the pore size distributions of the calcined powder and the pellet, uniaxially pressed at 500 MPa, are very similar (Fig. 2). The only change observed after uniaxial pressing is due to elimination of the pores larger than 10 nm. This means that relative dense packing is obtained already in the powder. Thus, the calcined powder consists of relatively dense packed crystallites and interparticle pores smaller than those particles. During compaction, the structure formed with closely packed primary particles is preserved and only some larger interagglomerate pores are eliminated due to fragmentation and rearrangement processes.

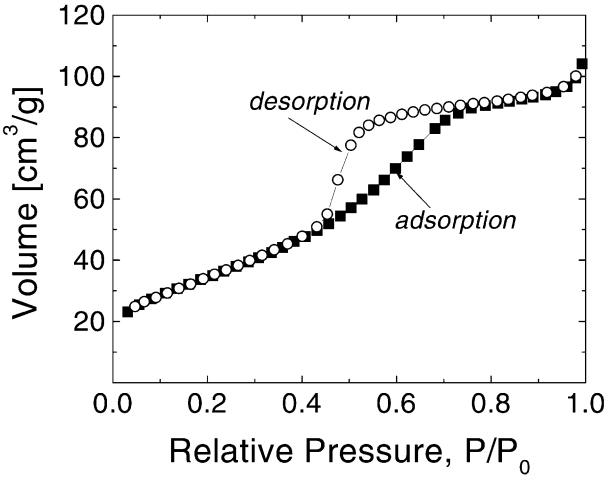

Fig. 1. Adsorption/desorption hysteresis loop of the calcined 3Y–TZP powder.

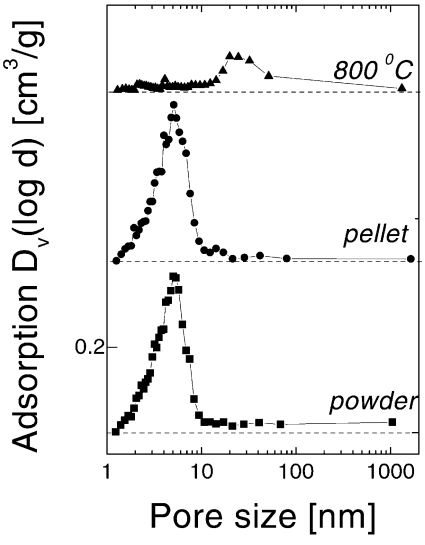

Fig. 2. Pore size distribution of 3Y–TZP calcined powder, pressed pellet and pellet air sintered at 800°C for 1 h.

The 3Y–TZP pellets were sintered in air at different temperatures up to 1070°C. The specific surface area and total pore volume decrease after air sintering at 800°C for 1 h, but an appreciable quantity of open pores still remains in the structure (Fig. 2). Simultaneously with grain coarsening, an increase of the average pore size is observed too (Fig. 2). Thus, a density higher than 90%TD can be achieved only with prolonged air sintering at 1070°C (Fig. 3). Densification of the 3Y–TZP is considerably improved by vacuum sintering, and a structure with closed pores is obtained after vacuum sintering at 1000°C for 1 h (Fig. 3). Better sinterability in vacuum than in air can be explained by a positive sintering pressure due to the removal of air and other adsorbents from the pores, enhanced particle repacking and enhanced diffusivity promoted by oxygen vacancies created under vacuum at high temperatures [13]. A high-resolution scanning electron micrograph of this sample (having 92.0%TD), presented in Fig. 4, shows uniform grain structures with a small portion of intergranular pores and the average grain size of about 100 nm.

3.2. Electrical conductivity

The impedance spectra of the zirconia stabilized with 3 mol% Y_2O_3 vacuum sintered at 1000°C for 1 h (having density of 92%TD) were measured in air and those obtained at 227, 376 and 527°C are presented in Fig. 5. According to the impedance spectroscopy measurement,

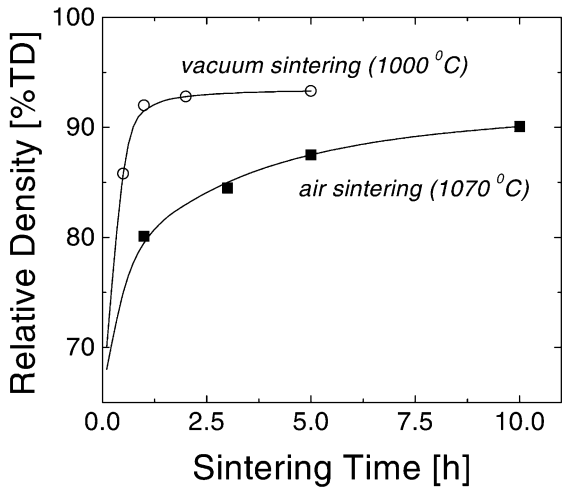

Fig. 3. Relative density as a function of sintering time.

three different regions could be resolved: (a) a high-frequency semicircle, due to the bulk resistivity and dielectric properties, (b) an intermediate-frequency semicircle, originating from the grain-boundary resistivity and (c) a low-frequency semicircle, ascribing ion and electron transfer at the surface contacting the electrode. It can be seen that all those semicircles may not be found at every spectra (selected measuring temperature) in the measured frequency range from 20 Hz to 3 MHz as the resistivity is strongly temperature dependent. The grain-boundary component of the total resistivity is dominant in those spectra indicating a low grain-boundary conductivity due to a high grain-boundary area, i.e. very small grain size. The electrical conductivity values derived from the impedance spectra obtained at different temperatures are presented in Table 2. The conductivity increases with temperature and the highest value of about 10^{-3} Ω^{-1} cm^{-1}, measured at 677°C, is in the range of the already published data [6,14].

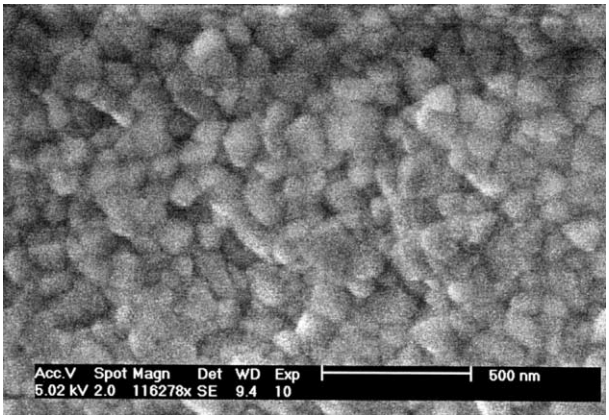

Fig. 4. HRSEM micrograph of 3Y–TZP vacuum sintered at 1000°C for 1 h.

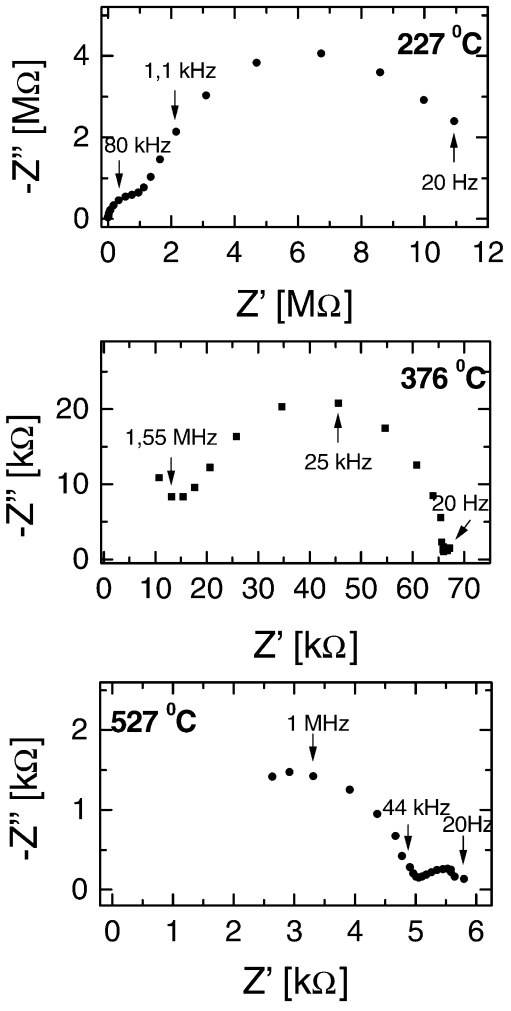

Fig. 5. Impedance spectra of 3Y–TZP vacuum sintered at 1000°C for 1 h.

Table 2
Conductivity of 3Y–TZP pellet vacuum sintered at 1000°C for 1 h (pellet density is 92.0%TD, pellet diameter is 6.10 mm and pellet thickness is 1.69 mm)

Measuring temperature (°C)	Total conductivity (Ω^{-1} cm^{-1})	Bulk conductivity (Ω^{-1} cm^{-1})	Grain boundary conductivity (Ω^{-1} cm^{-1})
76	–	3.98×10^{-10}	–
126	–	4.89×10^{-9}	–
176	–	2.37×10^{-8}	3.10×10^{-9}
227	4.69×10^{-8}	2.84×10^{-7}	5.10×10^{-8}
277	3.83×10^{-7}	1.24×10^{-6}	4.31×10^{-7}
327	2.37×10^{-6}	6.00×10^{-6}	3.00×10^{-6}
376	8.75×10^{-6}	–	1.13×10^{-5}
426	1.82×10^{-5}	–	2.30×10^{-5}
476	5.06×10^{-5}	–	6.07×10^{-5}
527	1.16×10^{-4}	–	1.56×10^{-4}
577	2.50×10^{-4}	–	–
627	5.01×10^{-4}	–	–
677	9.23×10^{-4}	–	–

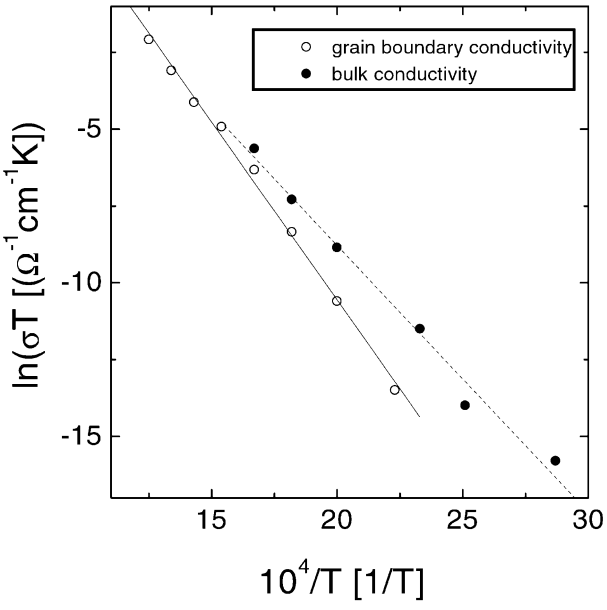

Fig. 6. Linear plot of $\ln\sigma T$ versus $10^4/T$.

The electrical conductivity results were analyzed by an Arrhenius equation of the form:

$$\sigma \cdot T = \sigma_0 \cdot \exp\left(\frac{-E}{kT}\right)$$

Fig. 6 shows the linear plot of $\ln\sigma T$ versus $104/T$. The activation energies of the bulk and grain-boundary conductivity are $E_b = 0.78$ eV and $E_{gb} = 1.00$ eV, respectively (with the corresponding pre-exponential factors of 7.6×10^3 and 3.1×10^5 Ω^{-1} cm^{-1}). Considerably higher activation energy of the grain-boundary conductivity is due to the very fine grain size and causes that the sol–gel derived zirconia stabilized with 3 mol% Y_2O_3 can be used in electrochemical devices, but only at relatively high temperatures.

4. Conclusions

(1) Zirconia stabilized with 3 mol% Y_2O_3 nanopowder has been synthesized by destabilization of an aqueous zirconia sol, prepared by alkoxide hydrolysis method.

(2) Zirconia ceramics with density higher than 92%TD and grain size of about 100 nm have been obtained by uniaxial pressing and vacuum sintering at 1000°C.

(3) The electrical conductivity of about 10^{-3} $\Omega^{-1}cm^{-1}$ at 677°C, together with quite high grain-boundary activation energy of 1.00 eV suggest that the dense zirconia stabilized with 3 mol% Y_2O_3 can potentially be used as oxygen semipermeable dense membrane, but only at relatively high temperatures.

Acknowledgements

The authors would like to thank the Alexander von Humboldt Foundation and the Thin Films Division group at Materials Science Department, Darmstadt University of Technology, Germany for help and support.

References

[1] S.P.S. Badwal, K. Foger, Solid oxide electrolyte fuel cell review, Ceram. Int. 22 (1996) 257–265.
[2] M. Filal, C. Petot, M. Mokchah, C. Chateau, J.L. Charpentier, Ionic conductivity of yttrium-doped zirconia and the composite effect, Solid State Ionics 80 (1995) 27–35.
[3] M.J. Verkerk, B.J. Middelhuis, A.J. Burggraaf, Effect of grain boundaries on the conductivity of high purity ZrO_2–Y_2O_3 ceramics, Solid State Ionics 6 (1982) 159–170.
[4] S.P.S. Badwal, Electrical conductivity of single crystal and polycrystalline yttria-stabilized zirconia, J. Mater. Sci. 19 (1984) 1767–1776.
[5] C. Petot, M. Filal, A.D. Rizea, K.H. Westmacott, J.Y. Laval, C. Lacour, R. Ollitrault, Microstructure and ionic conductivity of freeze-dried yttria-doped zirconia, J. Eur. Ceram. Soc. 18 (1998) 1419–1428.
[6] S.P.S. Badwal, J. Drennan, Grain boundary resistivity in Y–TZP materials as a function of thermal history, J. Mater. Sci. 24 (1989) 88–96.
[7] M.S. Kaliszewski, A.H. Heuer, Alcohol interaction with zirconia powders, J. Am. Ceram. Soc. 72 (6) (1990) 1504–1509.
[8] B.D. Cullity, Elements of X-ray Diffraction, Addison-Wesley, Reading, MA, 1978.
[9] E.P. Barrett, L.G. Joyner, P.P. Halenda, The determination of pore volume and area distributions in porous substrates. I. Computations from nitrogen isotherms, J. Am. Chem. Soc. 73 (1951) 373–380.
[10] Mondal, P. Elektrische Eigenschaften nanokristalliner Y_2O_3–stabilisierter ZrO_2–Keramiken, PhD thesis, Darmstadt, Germany, 1998.
[11] S. Lowell, J.E. Shields, Powder Surface Area and Porosity, 3rd Edition, Chapman & Hall, London, 1991.
[12] C.D. Sagel-Ransijn, A.J.A. Winnubst, A.J. Burggraaf, H. Verweij, The influence of crystallization and washing medium on the characteristics of nanocrystalline Y–TZP, J. Eur. Ceram. Soc. 16 (1996) 759–766.
[13] V.V. Srdić, M. Winterer, H. Hahn, Sintering behavior of nanocrystalline zirconia prepared by chemical vapor synthesis, J. Am. Ceram. Soc. 83 (4) (2000) 729–736.
[14] C.S. Chen, M.M.R. Boutz, A.J.A. Winnubst, B.A. Boukamp, A.J. Burggaaf, The electrical characterization of grain boundaries in ultra-fine grained Y–TZP, Mater. Sci. Eng. A 168 (1993) 231–234.